REMOTE OBSERVATION EXPERIMENT OF VOLCANIC ASH USING POLARIZATION LIDAR

Hamaki Inokuchi[1], Hiroshi Oikawa[1], Genta Morimoto[2] & Shigeru Inaka[1]

[1]Japan Aerospace Exploration Agency
[2]Metro Weather Co., Ltd

Abstract

Japan has many active volcanoes, some of which are located to the west of large cities. With prevailing westerly winds, there is a high probability that volcanic ash from their eruptions will affect those cities and their airports. There are also many active volcanoes near flight routes over the Pacific Ocean, and eruptions force more than flight 10 route changes each year. Although standards for limiting jet engine exposure to volcanic ash exist to minimize the risk to flight, they cannot be applied because satellite observations only observe the tops of ash clouds and cannot determine the volcanic ash mass concentration or the dispersion of ash in the atmosphere at different heights. The Japan Aerospace Exploration Agency (JAXA) is therefore developing an airborne volcanic ash detection lidar to remotely detect volcanic ash on airways and to determine its degree of hazard. Prior to volcanic ash observation flights, we conducted a ground-based observation experiment of volcanic ash at the Sakurajima volcano in Kagoshima Prefecture. The results indicated a correlation between the lidar received signal intensity and the mass concentration of volcanic ash in the atmosphere.

Keywords: Flight Safety, Volcanic Ash, Mass Concentration, Polarization Lidar, Sakurajima

1. Introduction

The risk that volcanic ash poses to jet engines is related to its mass concentration in the atmosphere and the exposure time, but the mass concentration on air routes is currently unknown. The dispersion area of a volcanic ash cloud is predicted from satellite observations and weather forecasts, but satellites can observe only the upper surface of the ash cloud, and so there is uncertainty as to extent of the cloud at each altitude between the top and the earth's surface. Even within expected areas of ash fall, there have been no actual measurements of volcanic ash mass concentration, and it is unknown quantitatively. For this reason, the Japan Aerospace Exploration Agency (JAXA) is developing a polarization lidar [1] that can be installed on aircraft to remotely observe volcanic ash and determine its level of hazard. Although this lidar is also being developed to observe ice crystals, at present we are focusing on confirming its volcanic ash observation function, given that the presence of continually active volcanoes in Japan makes it much easier to find suitable conditions for flight observations of volcanic ash than ice crystals. In this paper, we report on the flight test results of a volcanic ash sampling system developed for the calibration of the lidar, as well as the results of a ground-based volcanic ash observation experiment [2] conducted with the lidar at the Sakurajima volcano in Kagoshima Prefecture, as a prelude to flight observation tests.

2. Influence of Volcanic Ash on Aircraft

When volcanic ash enters a jet engine, it is melted by the heat of the engine and resolidfies on internal surfaces such as turbine blades and combustors, which is the main cause of engine failure. It also clogs filters, blocks fuel nozzles, and the hard, sharp ash particles also erode high-speed moving parts such as fan and turbine blades. The engine may need to be shut down in flight and replaced afterwards, posing a risk to safety and causing economic loss [3]. For this reason, flights currently avoid airspace where volcanic ash is observed by satellites, regardless of its concentration. A problem with satellite observations, however, is since they only observe the upper surface of the volcanic ash cloud, it is not possible to determine the distribution of ash below the cloud top. Also, when ash is observed near an airport, the safety impact on take-off and landing operations is unclear. When an eruption occurred in southern Iceland in April 2010, since the hazardous airspace could not be identified in detail, flight operations had to be completely suspended across Europe, resulting in huge economic losses. Moreover, volcanic ash sensors installed on satellites have become more sensitive in recent years and are now able to observe lower ash concentrations that, while they are not as hazardous, must still be avoided. For this reason, the operational costs due to excessively conservative ash avoidance are expected to increase in the future.

Regarding the risk that volcanic ash poses to flight, NASA in the United States conducted volcanic ash exposure tests using actual engines, and the results were published in 2017 [4]. In the same year, Rolls-Royce, which participated in the tests, proposed a volcanic ash exposure limit of 2 mg/m^3 × 2 hours = 14.4 g・s/m^3 as a standard value for flight. However, as there is currently no way to measure the mass concentration of volcanic ash on air routes, there is no way to comply with the standard.

3. Flight Test of Volcanic Ash Sampling System

To calibrate the remote observation polarization lidar, a sampling volcanic ash measurement system was developed and installed on a research helicopter to isokinetically sample [5] the atmosphere, measure the number concentration of aerosol particles in various size ranges using an Optical Particle Counter (OPC) and an Aerosol Monitor (AM) [6], and at the same time collect aerosol particles. Analyzing the components of collected particles and determining their specific gravities can be used to convert particle number concentrations to mass concentrations. In an ash sampling test flight conducted around an active volcano, however, the volcanic plume from the crater which was sampled was white and was estimated to be mostly steam. Since the particle number concentration data obtained by the OPC and AM from this test had large errors, they are omitted in this section, and the conversion method will be described in the section on ground-based tests.

3.1 Observation Flight Course

Two observation flights were conducted on January 27 and 28, 2021 around the Sakurajima volcano, Kagoshima Prefecture. The flight track of the January 27th observation flight is shown in Fig. 1. The helicopter took off from Kagoshima Airport and gradually approached the summit crater from the leeward side, repeatedly traversing the plume at 100 kt in a sinusoidal pattern.

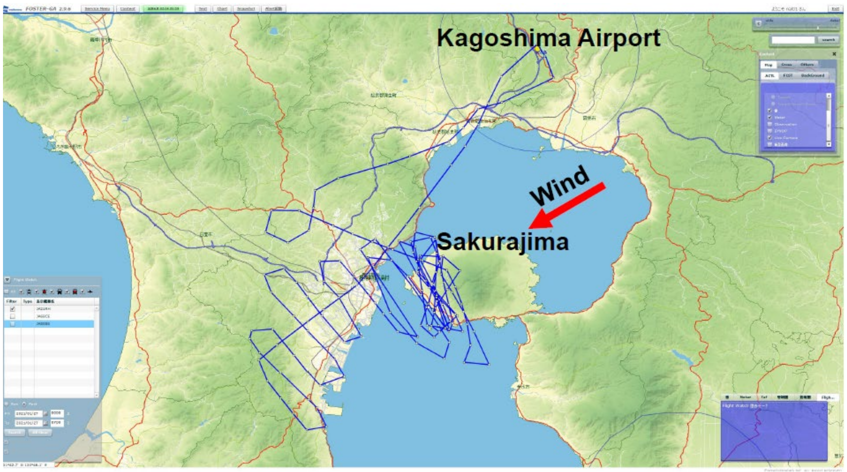

Figure 1 – Observation flight course.

3.2 Volcanic Ash Sampling

In order to estimate the mass concentration of volcanic ash by remote lidar observations and particle count sampling by OPC, it is necessary to determine the specific gravity of the ash. Fig. 2 shows example results of element analysis of materials collected in flight by a Multi Cascade Impactor (MCI) using a field emission-scanning electron microscope-energy dispersive X-ray spectrometer. Elements that are representative of volcanic ash, such as silicon, aluminum, potassium, magnesium, and oxygen were detected.

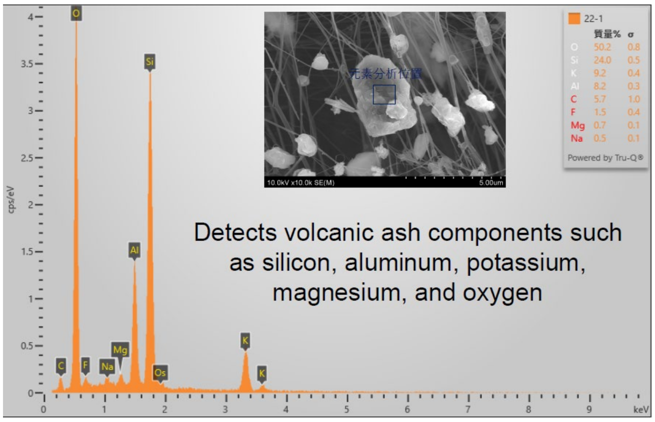

Figure 2 – Elemental analysis using an electron microscope.

The analyzed elements exist in volcanic ash as oxides, so their weight percentages as oxides were calculated by normalizing the atomic weight of the oxide divided by the atomic weight of the element and multiplying it by the weight percentage of the element. Finally, the specific gravity of the volcanic ash was then calculated by multiplying each known oxide density by its weight percentage and summing. The results are shown in Table 1.

Table 1 Specific gravity calculation.

Element	Na	Mg	Al	Si	K	Ca	Cr	Fe	Total
Oxide	Na_2O	MgO	Al_2O_3	SiO_2	K_2O	CaO	Cr_2O_3	FeO	
Density	2.27	3.65	4.00	2.33	2.32	3.37	5.21	5.90	
Weight %	7.3	1.5	20.6	56.4	5.1	6.1	0.2	2.8	100
Specific gravity	0.17	0.05	0.82	1.32	0.12	0.20	0.01	0.17	**2.86**

The specific gravity of the collected volcanic ash was calculated to be 2.86 [7]. However, since this analysis involved a small number of samples, and the chemical composition of volcanic ash varies depending on the origin of the magma, it would be premature to regard these results as standard values. Statistical processing based on future data accumulation is necessary, as well as data from other studies, such as that the work of Prata *et al.* into optical properties of volcanic ash from multiple volcanoes for remote sensing [8].

4. Polarization Lidar

Fig. 3 shows the principle of how a polarization lidar can estimate the material composition of airborne particles. Water droplets and small dust particles in the atmosphere are spherical, but volcanic ash and ice crystals are non-spherical. When a spherical particle is irradiated with a laser beam, the polarization of the transmitted light is maintained in the light scattered by the particle. In the case of non-spherical particles, however, the polarization of the scattered light changes, so by measuring the depolarization of the received light, it becomes possible to analyze the shape of the observed object; that is, to discriminate the target substance [9].

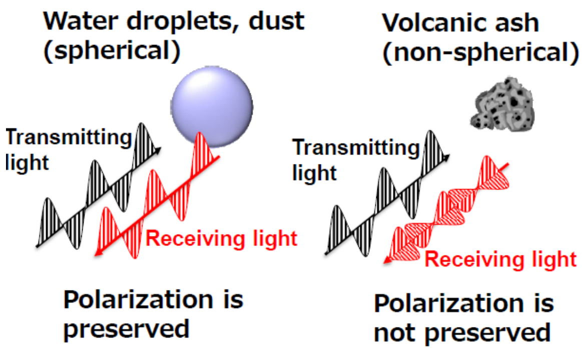

Figure 3 – Principle of polarization lidar.

It is assumed that the mass concentration of volcanic ash has a correlation with the scattering intensity of light it reflects, but the relationship is not necessarily linear. Therefore, we plan to calibrate the device from the perspective of identifying whether the mass concentration it is greater or less than 0.2 mg/m^3, which is an important threshold [10] for aircraft operations.

Figure 4 shows the configuration of the prototype polarization lidar, which is manufactured by Metro Weather. Laser light emitted from a Laser Diode (LD) is separated by a coupler into local light for taking beats in the receiving system and seed light for transmission. The seed light is frequency- and amplitude-modulated by an Acoustic Optical Modulator (AOM) and amplified by a Fiber Amplifier (FA). After the amplified light passes through a circulator, it is transmitted via a telescope into the atmosphere. Transmitted light back-scattered by particles in the atmosphere is received by the same telescope, and since the received light has P/S polarization, it is separated by a Polarization Beam Splitter (PBS), and each received light signal is detected by a photodetector as local light. Meanwhile, the beat signal is photoelectrically converted, and the beat and received light signals are processed by a Field Programmable Gate Array (FPGA) to obtain depolarization ratio and signal strength. A Personal Computer (PC) controls the polarization lidar and displays the acquired data.

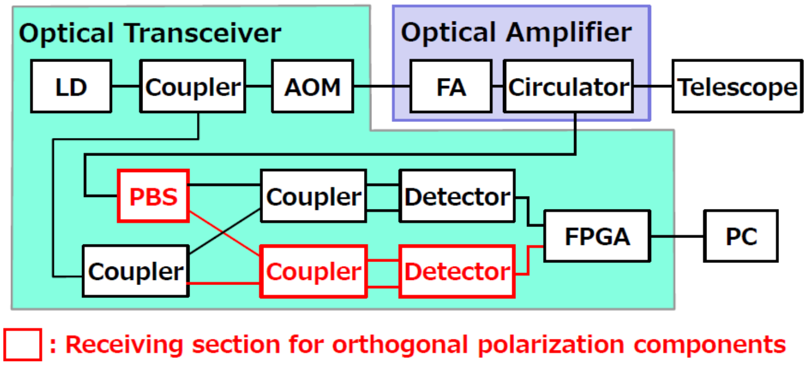

Figure 4 – Configuration of the polarization lidar.

Figure 5 shows a photograph of the prototype polarization lidar, and Table 2 shows its main specifications. The values other than the wavelength and telescope aperture diameter are those used in this experiment, but they can be changed. This polarized lidar is highly safe because it uses a laser with an eye-safe wavelength [11] of 1550 nm. It should be noted that since it was developed for the purpose of proving the ash measuring function, it is constructed from inexpensive commercially-available parts, and performance was not emphasized. In the near future, we plan to carry out observation flights with this prototype polarization lidar installed on a research helicopter, and we are working on downsizing the system to make it easier to install on aircraft.

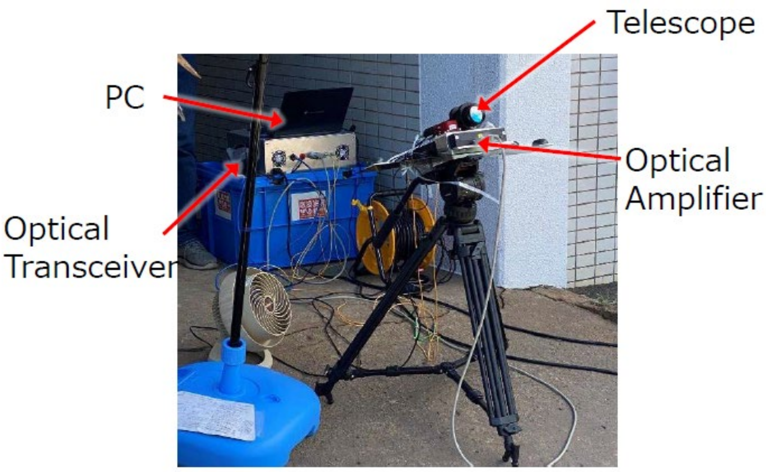

Figure 5 – Prototype polarization lidar.

Table 2 Specifications of the Polarization Lidar.

Transmission wavelength	1550 nm
Telescope aperture diameter	40 mm
Transmit pulse energy	100 μJ
Transmission pulse width	500 ns
Pulse repetition frequency	8 kHz
Output distance resolution	75 m

5. Ground Observation Experiment

5.1 Experimental site

The ground-based observation experiment was carried out from the Jigoku-gawara (riverbed of hell) site at Sakurajima on August 3 and 4, 2022, and observed the air volume between the site and the crater. During the previous week, on July 24, at around 8:05 p.m., a volcanic explosion projected a large volcanic block about 2.5 km east of the crater. As a result, the Kagoshima Local Meteorological Observatory raised the eruption alert level from 3 (mountain area entry restrictions) to the highest level 5 (evacuation). However, on the 27th, the level was lowered to 3, making it possible to conduct experiments, and the conditions were ideal for observation, with frequent small explosions and plumes constantly rising. The observation target this time was not the volcanic plume but an air volume in which volcanic ash could not be visually discerned. During the observation period, the weather was sunny and observations were made in the direction of blue sky.

5.2 Experimental Method

A polarization lidar receives light scattered from particles that are in the line of sight of the transmitted laser beam. Horizontally and vertically polarized backscattered light can be received simultaneously, and their ratio was calculated as the depolarization ratio and their sum was calculated as the received intensity every 10 seconds. However, since the received polarized light component orthogonal to the polarization of the transmitted light has low intensity and a lot of noise, in this experiment the intensity of the received signal was measured using only the same polarization component as the transmitted signal. Since the ultimate aim of the experiment was to estimate the mass concentration of volcanic ash from the received intensity, we first calculated the scattering intensity from the received intensity using a simple distance correction.

In order to measure the mass concentration of ash to serve as a reference for calibrating the polarization lidar, an OPC sensor was installed on a drone at a position where measurement is likely to be relatively unaffected by its propellers as shown in Fig. 6, and the particle number concentrations in various size ranges were acquired. The drone hovered at five points along the path of the polarization lidar's emitted beam and acquired data for 30 seconds at each point. However, since the lidar acquires data continuously, there was also data for the intervals when the drone was moving between the measurement points. Furthermore, since the influence of dynamic pressure on OPC suction is unknown, measurement errors may not be negligible.

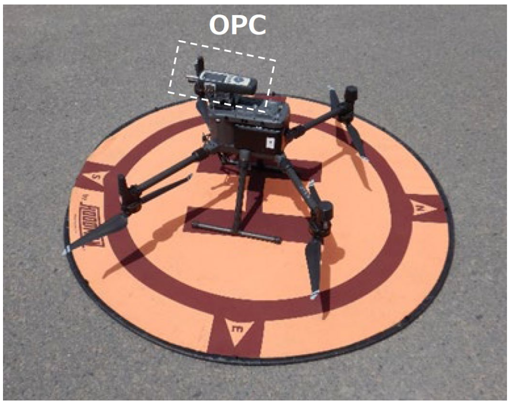

Figure 6 – OPC installation on a drone.

5.3 Measurement using OPC Installed on a Drone

The OPC used was a handheld type that can simultaneously measure the particle number concentrations in each of the following six particle diameter ranges every 30 seconds: greater than 0.3 μm, greater than 0.5 μm, greater than 1.0 μm, greater than 2.5 μm, greater than 5.0 μm, and greater than 10 μm. Figure 7 shows the measurement results. Although there is a higher concentration of smaller size particles, each particle diameter has similar the trends of concentration changes with time.

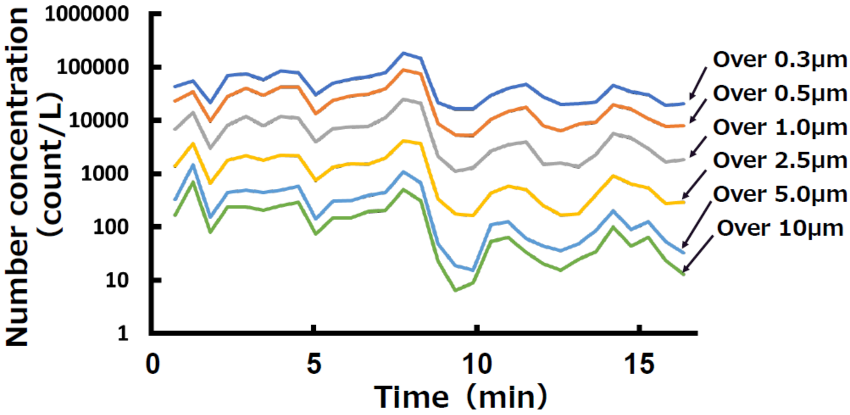

Figure 7 – OPC measurements.

Based on this result, for example, by subtracting the measured value of particles larger than 0.5 μm from the measured value of particles larger than 1.0 μm, it is possible to obtain the number concentration of particles between 0.5 and 1.0 μm in diameter. As there is no upper limit of the particle size defined for the concentration measurements of particles larger than 10 μm, it was assumed to be 20 μm since the particle size ranges are approximately equally spaced on a logarithmic scale. As an example, the number concentrations for each particle diameter range at a certain time are shown in Fig. 8.

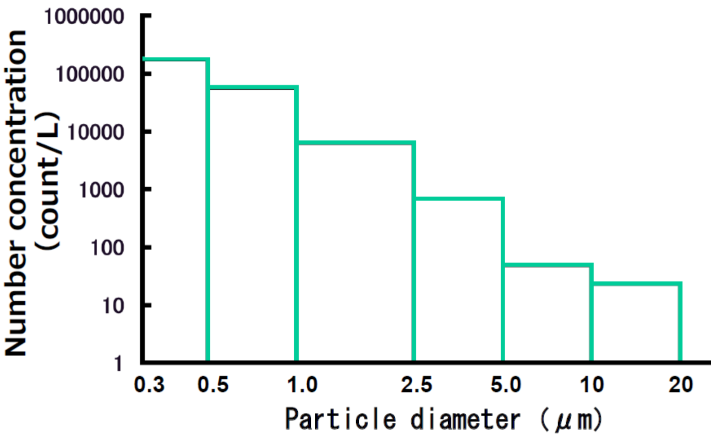

Figure 8 – Particle diameter distribution of number concentration by OPC.

The median value of each particle diameter range is herein referred to as the representative particle diameter. By assuming that all volcanic ash particles within the particle diameter range are spheres of the representative particle diameter, the volume concentration of each particle diameter range was first determined. Although actual volcanic ash particles are not spherical and the particle diameter defined by OPC is also only an average value, it was assumed that the resulting error would not be large. Next, the specific gravity of the particles was set to 2.86 based on the previous ash sampling flight results, and the particle diameter distribution of mass concentration was estimated as shown in Fig. 9.

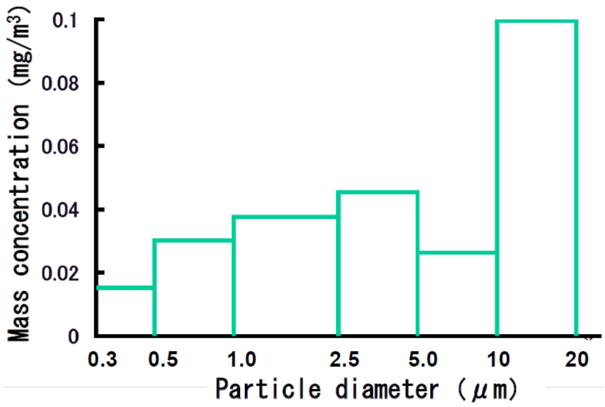

Figure 9 – Estimation of particle diameter distribution of mass concentration.

Substances with particle diameters of less than 1 μm are not volcanic ash, but are presumed to be particles of sulfuric acid and other substances that are secondary to volcanic gas [12]. Therefore, in calculating the mass concentration, the mass concentration of particles with a diameter of more than 1 μm was integrated, and in this example, a value of 0.209 mg/m^3 was obtained. Since the maximum particle diameter is assumed to be 20 μm, the fraction that this particle diameter range contributes to the calculation of mass concentration is large and could be a source of error. When the calculation was performed assuming maximum particle diameters of 15, 30 and 50 μm, the respective mass concentrations were 0.239, 0.201, and 0.208 mg/m^3, and thus it was found that no large error occurred.

5.4 Observation with Polarization Lidar

Figure 10 shows an example of an observation carried out at JAXA's Chofu Aerospace Center in Tokyo, which is assumed to be free of volcanic ash. The direction of observation was at an oblique angle above the horizon, and there may have been sand dust at low altitudes, but the light was hardly depolarized. In contrast, Figure 11 shows observation results at Sakurajima. The depolarization ratio due to volcanic ash is 0.4 to 0.6, and from the observed spatial density unevenness and its variation with time, it is inferred that an area of volcanic ash is being blown towards the observation site, even though it was a clear day, volcanic ash was not visible, there were no visible plumes in the observation direction, and it is possible to deduce from the depolarization ratio that there was little water droplet content.

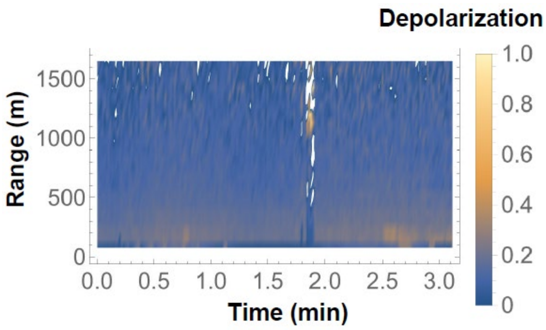

Figure 10 – Observation of ordinary atmosphere (JAXA Tokyo).

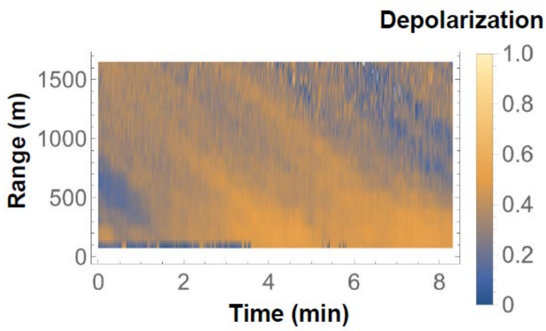

Figure 11 – Observation of atmosphere with volcanic ash (Sakurajima).

The laser beam emitted from the polarization lidar is scattered by volcanic ash, and it receives backscattered light is received. By subtracting the noise floor from the scattered light, a signal proportional to the received intensity is obtained. Even if the intensity of scattering is the same at all ranges, the received signal strength from ash at closer ranges will naturally be higher, and the strength from far ranges will be lower. Strictly speaking, it is therefore appropriate to solve the lidar equation [13] in order to determine the scattering intensity. For simplicity, we multiplied the received intensity by the square of the range and the reciprocal of atmospheric transmittance, since we considered range attenuation to be dominant. We considered the atmospheric transmittance to be 0.99998/m to the power of 2 times range [14]. In addition, for the purpose of comparison with the OPC observations of mass concentrations, we multiplied by a constant value as system factor, then raised the product to the power of 1.5 to calculate relative scattering intensity. The exponent value of 1.5 is because the mass concentration and scattering intensity of particles are proportional to the cube and square of particle diameter respectively. Figure 12 shows the relative scattering intensity due to volcanic ash obtained as described above, with the drone's flight course superimposed as a red line.

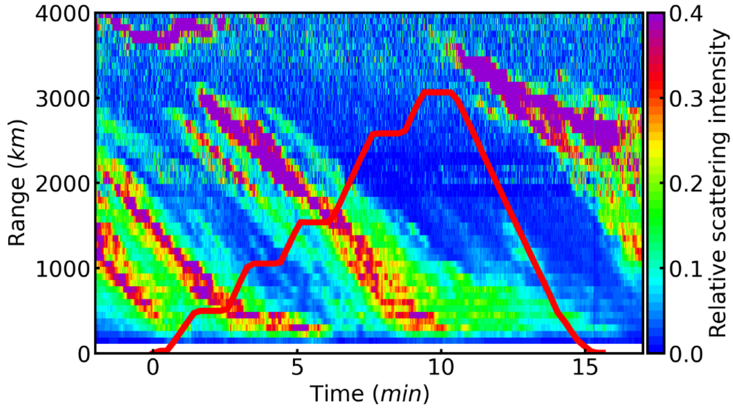

Figure 12 – Scattering intensity observation using polarization lidar.

Figure 13 shows a comparison between the relative value of the scattering intensity of volcanic ash by the polarization lidar at the drone's measurement position and the mass concentration of volcanic ash estimated from the OPC data measured by the drone. As can be seen in Figure 12, the volcanic ash concentration is highly uneven at locations where concentrations are high, and small differences in location or time can have in large differences in values. Although there is a shift in the peak values, there is an overall correlation between the polarization lidar and OPC measurements. Therefore, with appropriate calibration, it will be possible to estimate the mass concentration of volcanic ash in the atmosphere using the polarization lidar alone. The OPC data in Figure 13 shows a peak value at the beginning of measurement. This is due to drone's downdraft stirring up accumulated volcanic ash from the ground, which caused an increase in the measured mass concentration.

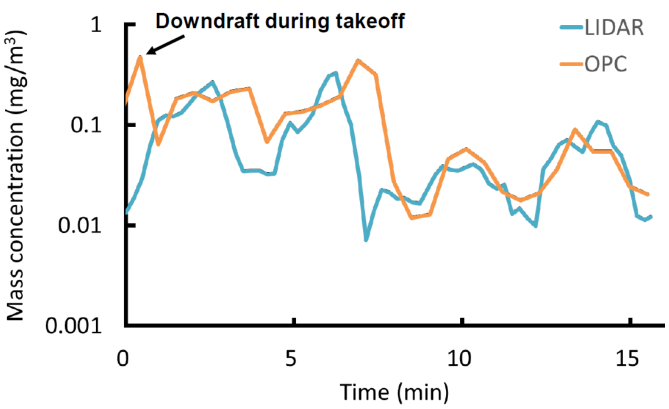

Figure 13 – Comparison of polarization lidar and OPC data.

6. Future plan

The OPC installed on the drone in this experiment was a modest device, so the measurement accuracy was low and the isokinetic sampling was not perfect. Moreover, since the spatial resolutions and sampling times of the OPC and lidar differed, it was difficult to make polarization lidar observations accurately at the drone's measurement position. In the near future, we plan to equip JAXA's research helicopter with both a high-precision OPC and a polarization lidar, and to conduct observation flights around Sakurajima to compare measurement data acquired simultaneously at the same locations by both systems. The installation work has already been completed, as shown in Figure 14, and an airworthiness test flight conducted on February 29, 2024 confirmed that there were no problems with the observation function. We are planning an observation flight at Sakurajima this winter.

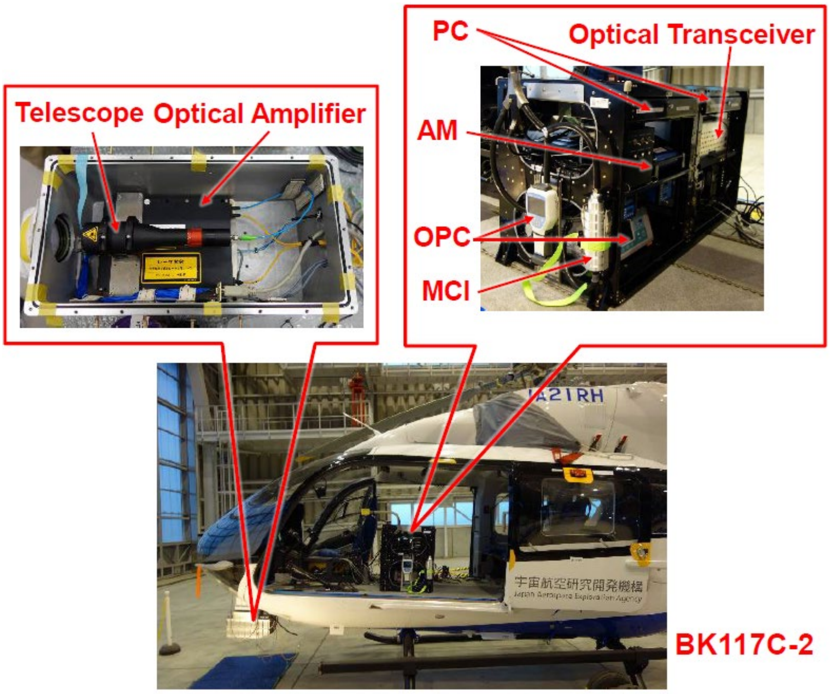

Figure 14 – Installation in a research helicopter.

7. Concluding Remarks

We conducted a ground-based volcanic ash observation experiment at the Sakurajima volcano, Kagoshima Prefecture using a polarization lidar designed for airborne applications, and the results are summarized below.

1) For the purpose of functional confirmation, we developed a prototype of an airborne polarization lidar from inexpensive commercially available parts. The lidar is highly safe because it uses a laser with an eye-safe wavelength of 1550 nm.

2) Using an OPC sensor mounted on a drone, we measured the number concentrations of volcanic ash particles in various particle diameter ranges, and estimated the ash mass concentration from the results.

3) The presence or absence of volcanic ash could be determined by the depolarization of back-scattered laser light measured by polarization lidar.

4) A correlation was found between the intensity of laser light scattering by volcanic ash measured by the polarization lidar and OPC particle concentration measurements. With appropriate calibration, it will be possible to estimate the mass concentration of volcanic ash in the atmosphere using the polarization lidar alone.

5) In the near future, we plan to install a high-precision OPC and polarization lidar in a research helicopter, and compare their simultaneous measurements in observation flights around Sakurajima.

8. Acknowledgment

In relation to this experiment, we would like to thank Professor Masato Iguchi of the Disaster Prevention Research Institute, Kyoto University, for suggesting observation locations and visiting Kyoto University's observation site on Sakurajima. Regarding the estimation of mass concentration of volcanic ash using the OPC, we received valuable suggestions from Associate Professor Tomoki Nakayama of the Faculty of Environmental Science, Nagasaki University. The effectiveness of the experiment was discussed by experts from the Lidar Review Committee. We would like to express our gratitude to those involved.

9. Contact Author Email Address

mailto: inokuchi.hamaki@jaxa.jp

10. Copyright Statement

References

[1] Hamaki INOKUCHI, Hiroshi OIKAWA, Nobuki KOTAKE: Feasibility study of an airborne volcanic ash and ice crystal detection lidar, *Proc. of the 57th Aircraft Symposium*, Yamaguchi, 3D11, 2019. (In Japanese).

[2] Hamaki INOKUCHI, Hiroshi OIKAWA, Takayuki NAKANO: Ground observation experiment of airborne volcanic ash and ice detection lidar at Sakurajima, *Proc. of the 61st Aircraft Symposium*, Fukuoka, 3B07, 2023. (In Japanese).

[3] Marianne Guffanti, Thomas J. Casadevall, and Karin Budding: Encounters of Aircraft with Volcanic Ash Clouds: A Compilation of Known Incidents, 1953–2009, Data Series 545, Version 1.0.

[4] John D. Lekki and Mark R. Woike: Vehicle integrated propulsion research (VIPR) III Volcanic ash ingestion testing, May 2017.

[5] Wilcox, J. D.: Isokinetic Flow and Sampling, *Journal of the Air Pollution Control Association*, 5:4, pp 226-245, 1956.

[6] Hamaki INOKUCHI, Hiroshi OIKAWA, Nobuki KOTAKE: Development of an Airborne Sampling Measurement System for Volcanic Ash, *Proc. of the 58th Aircraft Symposium*, Online, 3E01, 2020. (In Japanese).

[7] Hamaki INOKUCHI, Hiroshi OIKAWA, Takayuki NAKANO: Observation Flight of Aerosol Sampling around Sakurajima, *Proc. of the 60th Aircraft Symposium*, Niigata, 3A07, 2022. (In Japanese).

[8] G. S. Prata, L. J. Ventress, E. Carboni, T. A. Mather, R. G. Grainger 2, D. M. Pyle: A New Parameterization of Volcanic Ash Complex Refractive Index Based on NBO/T and SiO 2 Content, *Journal of Physical Research: Atmospheres*, Vol. 24, pp 1779–1797, 2019.

[9] Tetsu SAKAI, Tomohiro NAGAI, Narihiro ORIKASA, Yuji ZAIZEN, Katsuya YAMASHITA, Yuzo MANO, and Masataka MURAKAMI: Aerosol characterization by dual-wavelength polarization lidar measurements over Kochi, Japan during the warm seasons of 2008 to 2010, *JMSJ*, Vol. 91, No.6, pp 789-800, 2013-605, 2013.

[10] Rory Clarkson: Volcanic ash and aviation – *Rolls-Royce Position*, May 2017.

[11] Japan Standard Association. JIS C6802, 2018.

[12] Tomoki Nakayama: Observation of high concentration PM2.5 of volcanic origin in Nagasaki and Okinawa, *https://www.nagasaki-u.ac.jp/ja/science/science209.html*, 2020. (In Japanese).

[13] S. Kameyama et al.: Compact all-fiber pulsed coherent Doppler lidar system for wind sensing, *Appl. Opt,* 46, No.11, pp 1953-1962, 2007.

[14] Hamaki INOKUCHI, Tomohiro AKIYAMA: Performance Evaluation of an Airborne Coherent Doppler Lidar and Investigation of Its Practical Application, *Transactions of the Japan Society for Aeronautical and Space Sciences*, Vol. 65, Issue 2, pp 47-55, 2022.